Landfill cap models under simulated climate change precipitation:

Sinnathamby, G., Phillips, D., Sivakumar, V., & Paksy, A. (2014). Landfill cap models under simulated climate change precipitation: Impacts of cracks and root growth . *Geotechnique*, *64*(2), 95-107. https://doi.org/10.1680/geot.12.P.140

Published in:
Geotechnique

Document Version:
Publisher's PDF, also known as Version of record

Sinnathamby, G. *et al.* (2014). *Géotechnique* **64**, No. 2, 95–107 [http://dx.doi.org/10.1680/geot.12.P.140]

Landfill cap models under simulated climate change precipitation: impacts of cracks and root growth

G. SINNATHAMBY*, D. H. PHILLIPS*, V. SIVAKUMAR* and A. PAKSY†

Desiccation crack formation is a key process that needs to be understood in assessment of landfill cap performance under anticipated future climate change scenarios. The objectives of this study were to examine: (*a*) desiccation cracks and impacts that roots may have on their formation and resealing, and (*b*) their impacts on hydraulic conductivity under anticipated climate change precipitation scenarios. Visual observations, image analysis of thin sections and hydraulic conductivity tests were carried out on cores collected from two large-scale laboratory trial landfill cap models (~80 × 80 × 90 cm) during a year of four simulated seasonal precipitation events. Extensive root growth in the topsoil increased percolation of water into the subsurface, and after droughts, roots grew deep into low-permeability layers through major cracks which impeded their resealing. At the end of 1 year, larger cracks had lost resealing ability and one single, large, vertical crack made the climate change precipitation model cap inefficient. Even though the normal precipitation model had developed desiccation cracks, its integrity was preserved better than the climate change precipitation model.

KEYWORDS: landfills; microscopy; permeability; radioactive waste disposal; water flow

INTRODUCTION

Climate change impacts on waste management, particularly related to infiltration of rainwater through landfill caps protecting radioactive and other hazardous waste, is a growing concern. Thus, there is a need for landfill caps to be designed to endure impacts of future climatic scenarios. Weather/climate projection models for the UK show a high probability of wetter winters and drier summers in the next few decades due to global warming (Defra, 2009), which can lead to desiccation cracks in landfill caps. Although most modern landfill caps designed for radioactive and hazardous/industrial waste utilise geo-synthetic clay liners and geo-membranes to meet the minimum permeability criteria of 10^{-9} m/s (NRA, 1992; Jones *et al.*, 1993; SEPA, 2002), typically they also rely on naturally occurring low-permeability materials such as clays. However, caps composed of naturally occurring materials are prone to desiccation-induced cracking, which can compromise their integrity (Boynton & Daniel, 1985; Miller & Mishra, 1989; Montgomery & Parsons, 1989; Corser & Cranston, 1991; Basnett & Brungard, 1992; Basnett & Bruner, 1993; Melchior, 1997).

Costa *et al.* (2013) report that desiccation cracks in clays are controlled by flaws and/or pores in the material due to high suction stress, which results in sequential cracking, and Vallejo (2009) reports that fluid flow through clays is controlled by interconnected cracks. Cracks can also form quickly and grow in size over time. When crack formations in composite liners were studied by applying heat to soil samples, Bowders *et al.* (1997) reported a 20 mm deep crack formed on the first day, which eventually grew in depth to 150 mm after 8 weeks. In another landfill cap study where desiccation crack propagation from wetting and drying was examined, a severe crack that was about 10 mm wide after the first drying cycle reached a depth of 160 mm within a period of 170 h. Close to 90% of the desiccation cracking occurred within a 19 h period (Miller *et al.*, 1998). Rayhani *et al.* (2008) report that permeability increases for some highly plastic soils during cycles of wetting and drying are not significant, despite the presence of visible cracks after drying cycles. This is attributed to self-healing (resealing) of the cracks during wetting cycles and saturation. However, in a long-term study on a field-scale landfill cap in Germany, Melchior *et al.* (2010) reported no self-healing of desiccation cracks after rewetting from precipitation events.

In a long-term, 4-year study by Albright *et al.* (2006), in-situ and laboratory hydraulic conductivity (HC) tests carried out on a compacted clay barrier in a landfill cap before and after drought revealed an increase in HC by about three orders of magnitude, which was attributed to desiccation cracks. Also, the change in the pattern of the drainage from steady state to rapid and intermittent flow indicated that preferential flow paths or cracks formed due to desiccation. Dye tracer test and soil structure analysis confirmed the presence of cracks and roots in cracks. Albright *et al.* (2006) concluded that common surface processes, such as wetting and drying and root growth, caused extensive soil structure development and much higher drainage rates than expected. Taking into consideration the impacts of grass roots on landfill caps is important because grass is normally planted on landfill caps to protect the capping material from erosion; therefore, grass root penetration can also affect the HC of the caps (Melchior *et al.*, 1994; Bending & Moffat, 1997; Hutchings *et al.*, 2001; Albright *et al.*, 2006; Melchior *et al.*, 2010). Additionally, grass roots extract moisture from soil for transpiration. Because vegetation influences soil moisture, it could also play a major role in shrinking and swelling of expansive clays (Driscoll, 1983; Holtz, 1983; Hauser, 2008). Depletion of moisture from the ground leads to desiccation and eventually results in increased infiltration (Greenway, 1987). Lim *et al.* (1996) and Ng & Zhan (2007) report that roots can significantly increase matric suction (negative pore-water pressure) in soil by extracting water from it, and hence speed up the desiccation process.

Manuscript received 20 September 2012; revised manuscript accepted 5 November 2013. Published online ahead of print 23 December 2013. Discussion on this paper closes on 1 July 2014, for further details see p. ii.

* School of Planning, Architecture and Civil Engineering, Queen's University of Belfast, Belfast, Northern Ireland, UK.
† National Nuclear Laboratory, Chadwick House, Risley, Warrington, UK.

To the authors' knowledge, there are no studies in which the changes in HC of landfill covers have been explained through the combined effects of desiccation cracking, root growth and associated soil-structure changes, in response to climate change. The objectives of this study were to examine: (*a*) desiccation cracks and impacts that roots may have on their formation and resealing, and (*b*) their impacts on HC under anticipated climate change precipitation (CCP) scenarios in landfill cap models. This is the first study that reports desiccation crack formation and healing in landfill caps with regard to seasonal precipitation based on proposed future climate change scenarios.

MATERIALS AND METHODS

Landfill cap model construction and design

Two identical cap models were constructed as uniformly as possible by filling a custom-designed container with the soil layers as shown in Fig. 1. Italian ryegrass *Lolium multiflorum*, an annual/biennial grass with an extensive root system, was planted on a 30 cm thick topsoil layer (TSL) in the landfill cap models. This topsoil is commercially available and purchased from a local supplier. The topsoil contained about 10% organic matter (OM) which would help to support the ryegrass that was planted on the surface. This topsoil was also irradiated by the manufacturer in order to prevent the growth of weeds. A 30 cm thick, uniformly mixed subsoil layer (SSL) (mixture of 2:1 Belfast Sleech: coarse sand by dry weight to make a porous mixture) was emplaced directly beneath the topsoil layer to facilitate drainage.

Belfast Sleech is a Holocene age fine-textured, post-glacial, estuarine deposit, which underlies a large portion of Belfast City and its outskirts (Crooks & Graham, 1976). This material is fairly uniform and highly kneadable. Belfast Sleech has a notable amount of OM (Glossop & Farmer, 1979; Phillips *et al.*, 2011), as high as 6% (Phillips *et al.*, 2011), and also has plasticity limit of 21%, maximum moisture content of 55%, permeability of 10^{-10} to 10^{-11} m/s and optimum moisture content of 27·5% (Anderson, 2011). About 2 t of pure Belfast Sleech was mixed well before carefully packing into model containers to form the low-permeability layer (LPL). A 5 cm thick sand layer was placed below the LPL, followed by a 5 cm thick gravel layer to allow excess water to drain out of the boxes. Lateral drainage was only provided at the bottom and there was no lateral drainage in between layers. This is because, unless there is a flat/horizontal surface, it is difficult to ensure the uniform distribution of the static consolidation pressure which was applied after the construction of each layer.

These landfill capping models were held in large timber boxes (80 cm wide, 80 cm long and about 100 cm high) made of 25 mm thick wooden boards (Fig. 2(a)) and braced with steel frames. Box interiors were coated several times with water-resistant paint to prevent water leakage. Holes drilled in the bottom of the boxes allowed excess water to drain. At interfaces between each layer, 'L' flanges were attached to the sides of the boxes to prevent preferential flow of water at the edges of the cap material.

The filling/construction of the TSL, SSL and LPL was carried out in several 50 mm thick layers. However, the Belfast Sleech contained small traces of mollusc shells, which were removed while kneading and packing in storage bags. This was laborious and it was impossible to remove all of the small shells from the large amount of Belfast Sleech used in the capping layers. Therefore, water content and particle size analysis were chosen as deciding parameters of homogeneity and uniformity of the material. From randomly collected samples of material prior to placement in the 50 mm thick layers, particle size analysis by hydrometer (BS 1377: Part 2, Method 9.2 (BSI, 1990a)) and moisture content (BS 1377: Part 2, Method 3 (BSI, 1990a)) tests were conducted to confirm uniformity of the material. The TSL, SSL and LPL were subjected to static loading prior to the placement of the subsequent layer. After each layer was packed into the boxes, they were subjected to static loading to generate a vertical pressure of 10 kPa by placing concrete blocks, each weighing 20 kg in a symmetrical manner. These blocks were stacked on a wooden plate (790 mm × 790 mm) located at the top of the layer. Gunny bags were placed in between the wooden plate and the soil to prevent the plate from sticking to the capping material and to dissipate excess water during loading. This ensured easy removal of the loading plate during the unloading. Dial gauges were fixed at the sides of the timber boxes, and settlement was monitored at regular intervals. When the settlement ceased, the concrete blocks were removed. There was no dynamic compaction involved during the compaction of the cap.

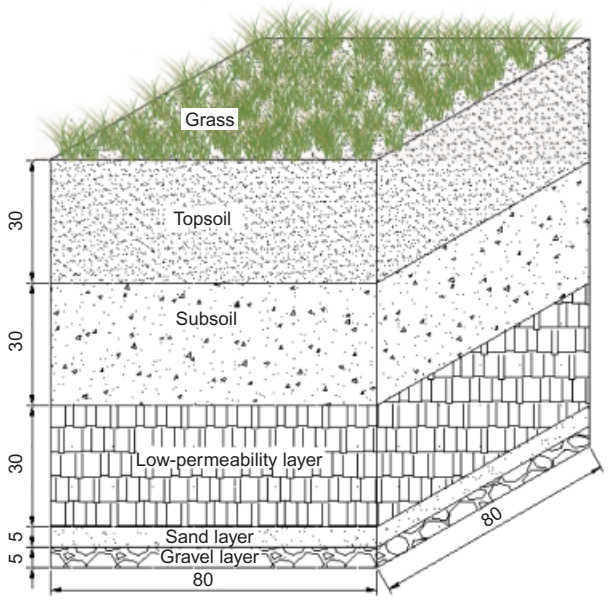

Fig. 1. Landfill capping layers in this study (dimension in cm)

Simulated precipitation

The two landfill cap models underwent simulated precipitation for seasonal durations of winter, spring, summer and autumn over a 1-year period (Table 1). Daily precipitation for the normal precipitation cap (NP) model was based on data from the UK Met office for Cumbria, Lake District for Eskmeals, collected over 29 years from 1971 to 2000. Eskmeals was selected as this is the nearest weather station to the UK's only low level waste repository (LLWR), near Drigg. Precipitation conditions for the CCP model were based on weather/climate projection models for the UK with a high probability of wetter winters and drier summers in the next few decades due to global warming (Defra, 2009). As a reasonable assumption, 15% increase in winter precipitation and 15% deficit in spring and autumn precipitation was used. Also, the CCP model underwent an extreme deficit of summer precipitation to investigate resealing of capping layers in subsequent wetting cycles.

The amount of precipitation for each season was distributed evenly throughout the season by sprinkling water evenly across surface of the landfill caps. Precipitation events were simulated to occur twice a week during the spring and summer periods (as the precipitation was relatively low) and

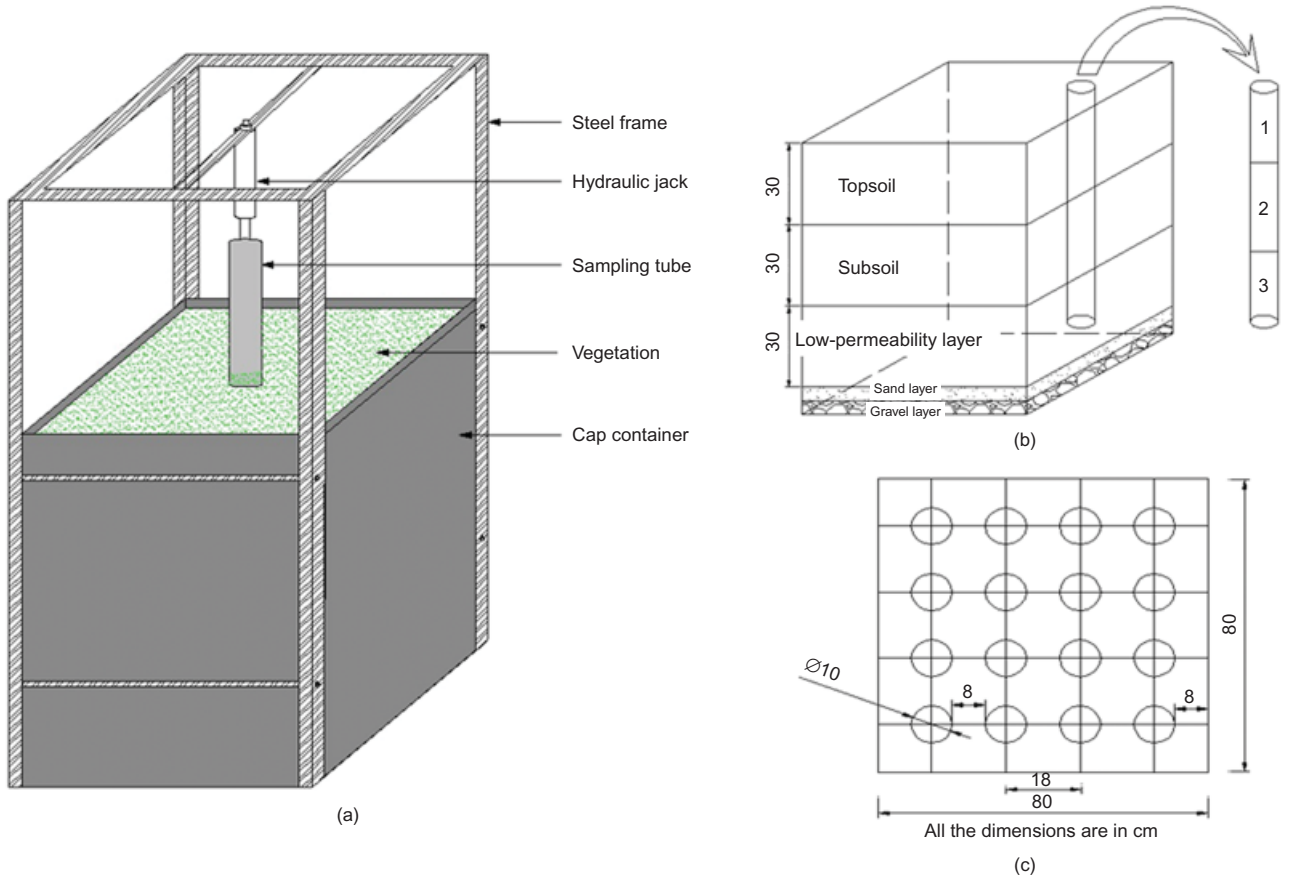

Fig. 2. Diagrams showing (a) the container and sampling set-up with hydraulic jack; (b) a vertical view of core collection; (c) a horizontal view of the sampling scheme

Table 1. Simulated seasonal precipitation carried out over a 1-year period in the present study

Season	Months	Mean monthly precipitation: mm	
		Normal precipitation cap (NP)	Climate change precipitation cap (CCP)
Winter	December, January, February	97	112*
Spring	March, April, May	65	55†
Summer	June, July, August, September	80	10‡
Autumn	October, November	109	125*

* 15% increased rainfall as per climate projections.
† 15% reduced rainfall as per climate projections.
‡ Continuous dry days with less rainfall.

three times a week during autumn and winter periods (as the precipitation was heavier during these periods), and the amount of precipitation was calculated based on the precipitation frequency. Frequency of precipitation events was carefully selected to avoid any ponding of water at the top and base of the cap and also to provide/maintain enough moisture in the cap despite the evaporation. Evaporation from the caps was constant throughout the testing period, because the testing programme was carried out in a controlled environment. The landfill cap models were stored in a greenhouse at a constant temperature of 20°C (±2) and constant relative humidity of 95%.

Landfill cap model sampling

Before the cores were collected from the large-scale physical landfill cap models, a small-scale cap model was constructed to practice: (*a*) how to pack the clay layers homogeneously without entrapping air and voids, (*b*) how to sample with minimal disturbance to the surrounding area of the cap and (*c*) how to refill capping material into the core.

Cores from the landfill cap model were collected at the end of every simulated season. Two cores (~100 mm dia.), one for the permeability test and the other for thin sections, were collected at the same time from each large-scale landfill cap model. A control core was also collected as soon as the cap was constructed (before the start of the simulated precipitation). Before each sampling event the surface of the landfill cap was slightly wetted to improve penetration through any crust that had formed on the surface of the cap, especially during drier simulated seasonal events. A specialised sampling tube with a height of approximately 1 m and an internal core diameter of 102 mm was designed to avoid/minimise disturbance to surrounding soil when collecting cores from the landfill cap models. The tube was constructed from stainless steel with a tapered cutter at the drilling end (Figs 3(a) and 3(b)). This cutter was designed with a sharp edge so that it could be driven into the cap easily to

minimise disturbance of surrounding sediments. The clearance of 0·5 mm between the cutter and the outer face of the tube reduces skin friction with the clay to make the extraction process easier (Figs 3(a) and 3(b)). There is a slight possibility that some cracks may have occurred in the core during extraction; however, the cores were collected as gently as possible and care was taken during preparation of the core material for analysis and thin sections to avoid any disturbances that could lead to cracking.

A hydraulic jack was used to drive the sampling tube into the caps (Figs 2(a)–2(c); Sinnathamby, 2011). All of the samples were stored at 10°C (±1). The empty bore holes were immediately refilled after sampling with similar pre-prepared landfill capping materials as precisely as possible to match up with the adjacent layer material in the model, to maintain moisture content of the cap material and to reduce pooling of water in the holes. The material was added very carefully so as not to disturb the rest of the model. The sections of the model, where the cores were taken, were not resampled and were left to reform as part of the model.

Thin section production and analysis

The acetone replacement method according to MacLeod (2008) was used to impregnate the core material. Soil thin sections were made and analysed (Sinnathamby, 2011) and described according to Fitzpatrick (1993). Desiccation crack behaviour and formation were studied in thin sections using a Zeiss Axioskop 40 petrographic microscope equipped with a Pixera Pro 600ES (DiRector™) digital camera connected to a computer with Image-Pro Plus® 7 image analysis software programme. Selected areas of thin sections were analysed to examine the mineralogy using a Philips scanning electron microscope (SEM) equipped with an Oxford Instruments energy-dispersive X-ray spectroscopy (EDS) micro-analyser after they had been carbon coated using an agar carbon coater. According to Phillips *et al.* (2011), X-ray diffraction analysis detected quartz, orthoclase, pyroxenes, spalerite, pyrite, calcium carbonate (shell fragments) in silt and sand fractions in Belfast Sleech, while the clay-size fraction (<2 μm) contained kaolinite, illite, chlorite and smectite. Smectite can swell when soil is wetted, causing cracks to close, which makes it an attractive material for landfill caps and lining material (Phillips *et al.*, 2011).

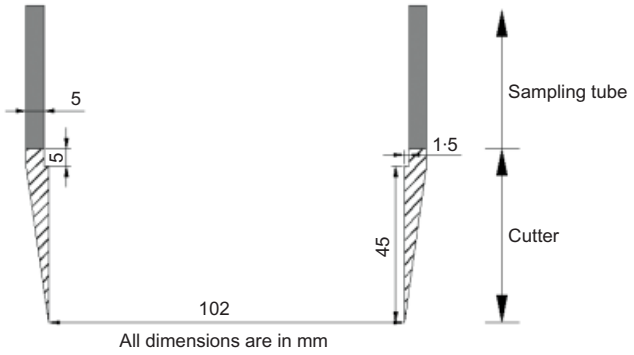

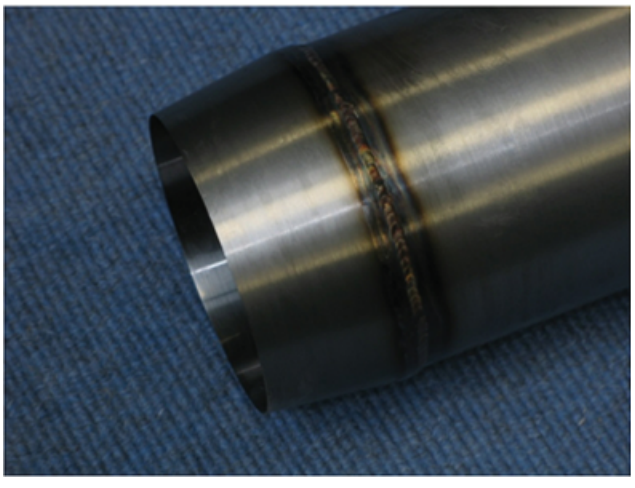

Fig. 3. (a) Design of the tapered cutter showing sharp edges and the clearance (gap) between the cutter and the outer face. (b) Tapered cutter at the drilling end of the sampling tube

Hydraulic conductivity tests

Three samples, one from each layer, were taken from cores for HC testing. The constant head HC test was carried out for each of these samples using the equipment set-up given in BS 1377, Part 6 (BSI, 1990b), with a tri-axial cell and three automatic pressure and volume control units (APCs) (Tables 2 and 3). Sample dimensions were 100 mm dia. and 100 mm high. Prior to measurement, the sample was saturated according to BS 1377, Part 6 (BSI, 1990b). All tests were conducted over a 5-day-long permeability stage under the following stress conditions: average consolidation pressure of 30 kPa and head difference of 10 kPa. Rate of flow through the sample was used for determining the permeability value.

RESULTS AND DISCUSSION

Visual (field) observations of impacts of simulated seasonal precipitation on desiccation crack formation and root growth

At the beginning of the study, both cap models were prepared in an almost identical way; therefore, similar observations were made for them during the initial sampling round soon after their construction. The TSL was loose, grass roots were absent and only fine fissures were observed in the caps during the initial phase of the study. The NP cap model underwent a regular mean monthly winter precipitation of 97 mm for about 3 months, whereas the CCP model experienced an increased winter precipitation of 15% (112 mm). An extensive amount of roots had grown in the first 3-month period and were found in the upper 5–10 cm of the TSL of both cap models (Figs 4(a) and 5), as also reported in a study by Hauser (2008). No signs of cracks were observed throughout both cap models. Minor fissures observed in the previous cycles had disappeared due to the swelling of OM and smectite in the clay fraction upon wetting in both cap models (Figs 5, 6(a) and 6(b)).

Table 2. Specifications of the tri-axial cell and automatic pressure control (APC) units

Specifications	Measurements
Tri-axial cell	
Maximum specimen size ($D \times H$)	10 cm × 10 cm
Internal volume	$1{\cdot}92 \times 10^6$ mm^3
Internal dimensions ($D \times H$)	12 cm × 17 cm
External dimensions ($D \times H$)	17 cm × 19 cm
Automatic pressure control units	
Medium	De-aired water
Maximum pressure	3000 kPa
Resolution of pressure measurement	±1 kPa
Resolution volume	±0·001 ml
Dimensions ($L \times B \times H$)	65 cm × 20 cm × 15 cm

Table 3. Hydraulic conductivity testing conditions and results

Sample	Pressures			Mean effective stress: kPa	Hydraulic gradient	Degree of saturation: %	Permeability: m/s
	Cell: kPa	Inlet: kPa	Outlet: kPa				
Initial sampling							
NP TSL	600	575	565	30	10	96	$6{\cdot}31 \times 10^{-8}$
NP SSL	500	475	465	30	10	98	$2{\cdot}57 \times 10^{-10}$
NP LPL	500	475	465	30	10	99	$2{\cdot}58 \times 10^{-10}$
CCP TSL	600	575	565	30	10	96	$5{\cdot}95 \times 10^{-8}$
CCP SSL	500	475	465	30	10	98	$2{\cdot}55 \times 10^{-10}$
CCP LPL	500	475	465	30	10	99	$2{\cdot}54 \times 10^{-10}$
After winter cycle							
NP TSL	–	–	–	–	–	–	–
NP SSL	500	475	465	30	10	99	$1{\cdot}96 \times 10^{-9}$
NP LPL	500	475	465	30	10	100	$9{\cdot}73 \times 10^{-10}$
CCP TSL	–	–	–	–	–	–	–
CCP SSL	500	475	465	30	10	99	$7{\cdot}03 \times 10^{-10}$
CCP LPL	500	475	465	30	10	100	$5{\cdot}67 \times 10^{-10}$
After spring cycle							
NP TSL	600	575	565	30	10	96	$1{\cdot}19 \times 10^{-7}$
NP SSL	500	475	465	30	10	97	$1{\cdot}65 \times 10^{-8}$
NP LPL	500	475	465	30	10	98	$2{\cdot}83 \times 10^{-9}$
CCP TSL	600	575	565	30	10	96	$1{\cdot}27 \times 10^{-7}$
CCP SSL	500	475	465	30	10	98	$3{\cdot}85 \times 10^{-9}$
CCP LPL	500	475	465	30	10	99	$1{\cdot}09 \times 10^{-8}$
After summer cycle							
NP TSL	600	575	565	30	10	95	$1{\cdot}30 \times 10^{-7}$
NP SSL	500	475	465	30	10	96	$4{\cdot}42 \times 10^{-8}$
NP LPL	500	475	465	30	10	97	$2{\cdot}47 \times 10^{-10}$
CCP TSL	600	575	565	30	10	95	$1{\cdot}29 \times 10^{-7}$
CCP SSL	500	475	465	30	10	96	$6{\cdot}52 \times 10^{-8}$
CCP LPL	500	475	465	30	10	97	$6{\cdot}34 \times 10^{-8}$
After autumn cycle							
NP TSL	600	575	565	30	10	95	$1{\cdot}35 \times 10^{-7}$
NP SSL	500	475	465	30	10	96	$1{\cdot}85 \times 10^{-8}$
NP LPL	500	475	465	30	10	97	$4{\cdot}98 \times 10^{-10}$
CCP TSL	600	575	565	30	10	97	$1{\cdot}16 \times 10^{-7}$
CCP SSL	500	475	465	30	10	96	$1{\cdot}85 \times 10^{-8}$
CCP LPL	500	475	465	30	10	96	$2{\cdot}80 \times 10^{-10}$

After the spring precipitation (65 mm/month), desiccation crack formation was barely noticeable in the NP model layers as they retained sufficient moisture in this cycle. The CCP model experienced a 15% deficit in mean monthly precipitation (55 mm) and minor desiccation cracks were observed in its core samples. Grass roots began penetrating into the subsoil in both cap models (Figs 4(a) and 5). This is consistent with findings from Hauser (2008), who observed that root distribution may shift downward towards wet layers, where the plants search for moisture when the topsoil is dry. Italian ryegrass was used in this study as it is grown on landfill caps (Albright *et al.*, 2004), because it establishes quickly and has well-developed root growth which holds soil in place to prevent erosion.

The NP model was subjected to a typical mean monthly summer precipitation of 80 mm resulting in only small narrow macro-cracks (width ranging from 0·5 to 6 mm), compared to larger cracks observed in the CCP model. In the simulated summer precipitation event, the CCP model was subjected to an extreme drought with only about 5 mm precipitation for 3 months. The TSL developed a surface crust and excessive moisture loss made the soil material in this layer very hard and more brittle (Fig. 5). Although a similar grass roots distribution was observed in the CCP model as that found in the NP model during this period (Fig. 5), grass roots penetrated down to the LPL through wide, open desiccation cracks ranging from 0·5 to 8 mm wide throughout the CCP cap (Figs 4(b) and 5). Albright *et al.* (2004) report that roots penetrate into cracking planes because they can more easily absorb soil moisture in these void spaces and move more freely, which can cause further cracking of the clay layer. Small, white, enchytraeid worms, commonly found in natural soils (Phillips & FitzPatrick, 1999), were observed feeding on the roots in the cracks.

During the autumn cycle, the NP model experienced the typical 109 mm/month precipitation compared to the CCP model, which was subjected to a 15% increased mean monthly precipitation of 125 mm. After the cycle, relatively small macro-cracks that remained unsealed in the SSL and the LPL were observed in the NP model. However, the

(a)

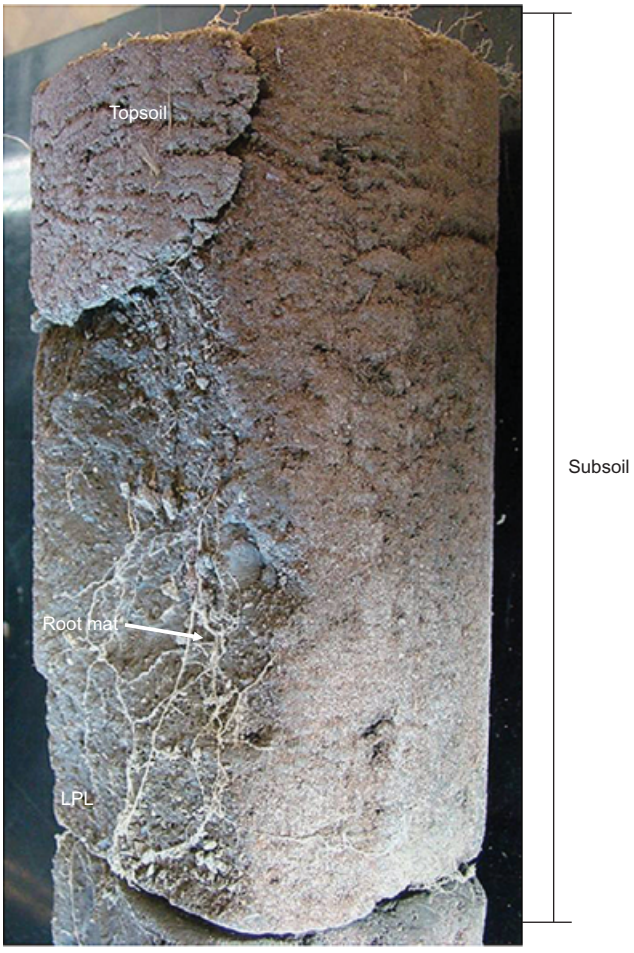

(b)

Fig. 4. Cores from the landfill cap models showing: (a) grass roots at the interface of topsoil and underlying subsoil after the spring cycle in the NP model; (b) a root mat along a deep crack in the subsoil of the CCP model after the summer cycle drought

dimensions and the severity of cracking were mild compared to the CCP model. Continuous moisture retention in the NP model preserved the subsoil layer from extensive cracking. The CCP model in this study developed desiccation cracks ranging in width from 2 to 10 mm, which remained unsealed after several cycles of wetting and drying. A major desiccation crack formed in the CCP model from the top of the subsoil to the bottom of the LPL, with widths exceeding 15 mm at some locations making the cap ineffective. Similar to a study by Yesiller *et al.* (2000), dimensions and patterns of cracks that (*a*) penetrated the entire upper layer and continued into the lower layers; (*b*) penetrated the entire upper layer, but did not continue into the lower layers; and (*c*) partially penetrated each layer were observed in the CCP model in the present study. However, in the NP model, the majority of cracks developed only partially penetrated each layer. Cracking of the barrier layers in a landfill cap can decrease the function of the cap and jeopardise the integrity of the whole containment system owing to increased infiltration (Miller *et al.*, 1998). Yesiller *et al.* (2000) reported a similar observation in landfill caps where desiccation cracks penetrated the entire depth of a 180 mm compacted clay cover. The cracks in SSL and LPL also show different directional patterns. This type of desiccation-induced crack patterns may be largely attributed to the clay content of these two soil layers as reported by Yesiller *et al.* (2000), Tay *et al.*, 2001, Boivin *et al.* (2004) and Tang *et al.* (2008). Shrinkage-induced cracking also increases with increased fines content (Yesiller *et al.*, 2000; Tay *et al.*, 2001). Also, the number of cracks were fewer and the dimensions of the cracks formed in the upper layers were less than the number and the dimensions of cracks present in the LPL of both CCP and NP models (Fig. 5). Yesiller *et al.* (2000) suggest that this is because the high sand content, which was present in the upper layers of the cap models, does not allow for extensive cracking. When a clay/sand mixture (sandy clay) experiences drought conditions, it does not easily crack under an environment of mild desiccation. However, if a sandy clay cracks under severe drought conditions, it will completely lose its resealing capacity. This clearly explains the reason behind the major crack that penetrated the entire depth of the CCP model. The severe drought condition experienced by the CCP model in the summer cycle resulted in cracking of the SSL first and the subsequent moisture loss from the LPL through these opened cracks eventually led to cracking along the same plane where the SSL cracked.

After the autumn precipitation event, grass roots strengthened the topsoil in both caps, and in the CCP cap they penetrated to the bottom of the model through the void spaces and were beginning to spread throughout the cracks. Root development in CCP and NP models was very dense in the upper 20–30 cm; however, some roots penetrated as deep as 50–55 cm in the CCP model, which is similar to observations of Montgomery & Parsons (1989). The amount of root mass in each layer decreased with the depth, as observed in Albright *et al.* (2004) and Montgomery & Parsons (1989). However, in a longer study (8 years), Melchior (1997) reported roots creating cracks and penetrating down the entire landfill cover. After a severe summer drought, active roots were also deep in the CCP model cover where the soil was moist. These barrier layers are vulnerable to root penetration, and eventually after cycles of wetting and drying which create zones of weakness, roots can easily penetrate the entire depth of the covers.

Impact of desiccation cracks and root growth on hydraulic conductivity

Topsoil layers. The TSL was rich in OM (10–15%), and owing to the excessive water content in the samples and the softness of the soil, it was difficult to obtain a sample for the HC test after the winter cycle in which the caps were subjected to heavy wetting. Similarly, Yesiller *et al.* (2000) reported soil softening and strength decrease due to wetting of a landfill cap. Unlike the SSL and LPL, the TSL was rich

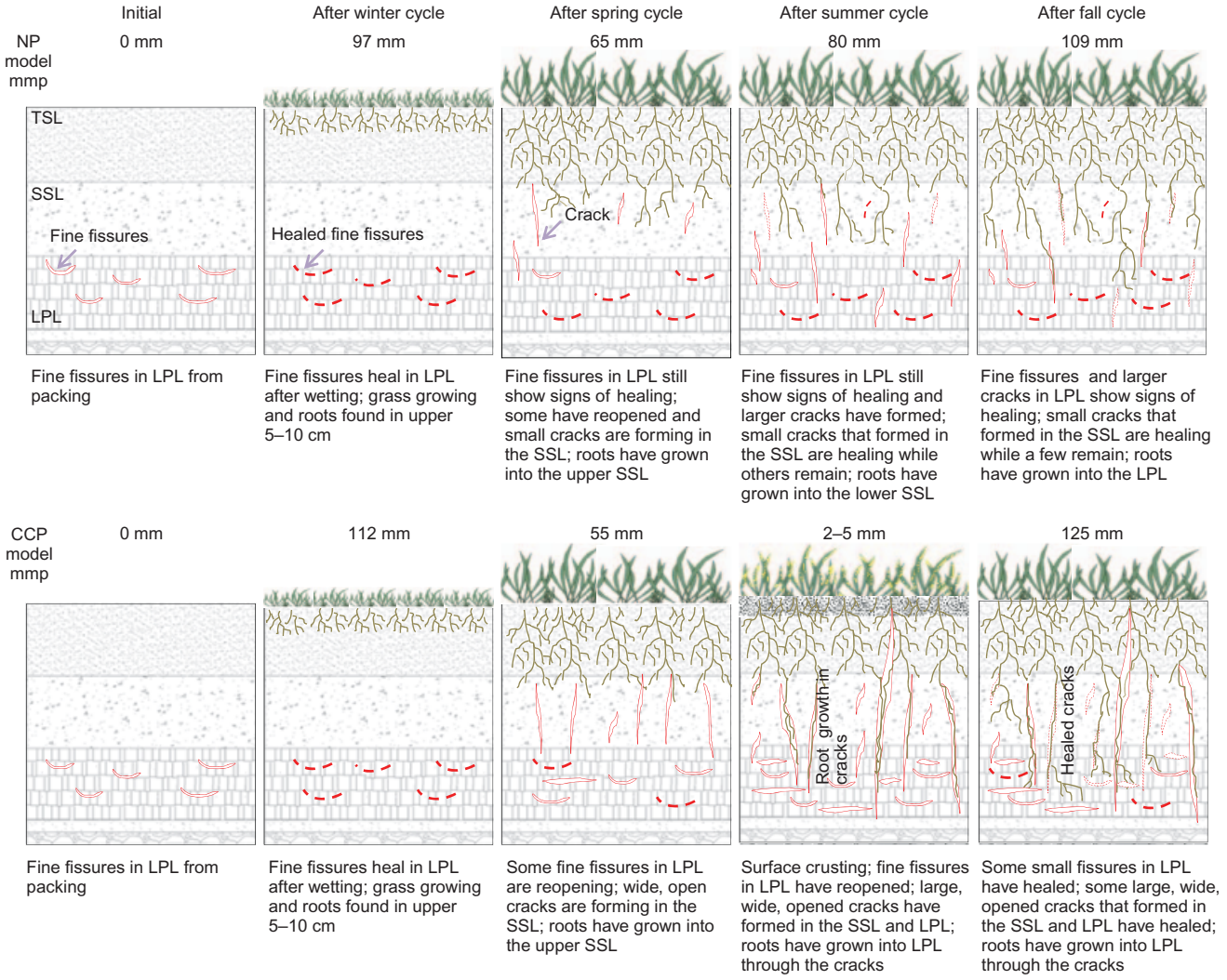

Fig. 5. Conceptual model of crack formation and root growth in the landfill cap models used in the study

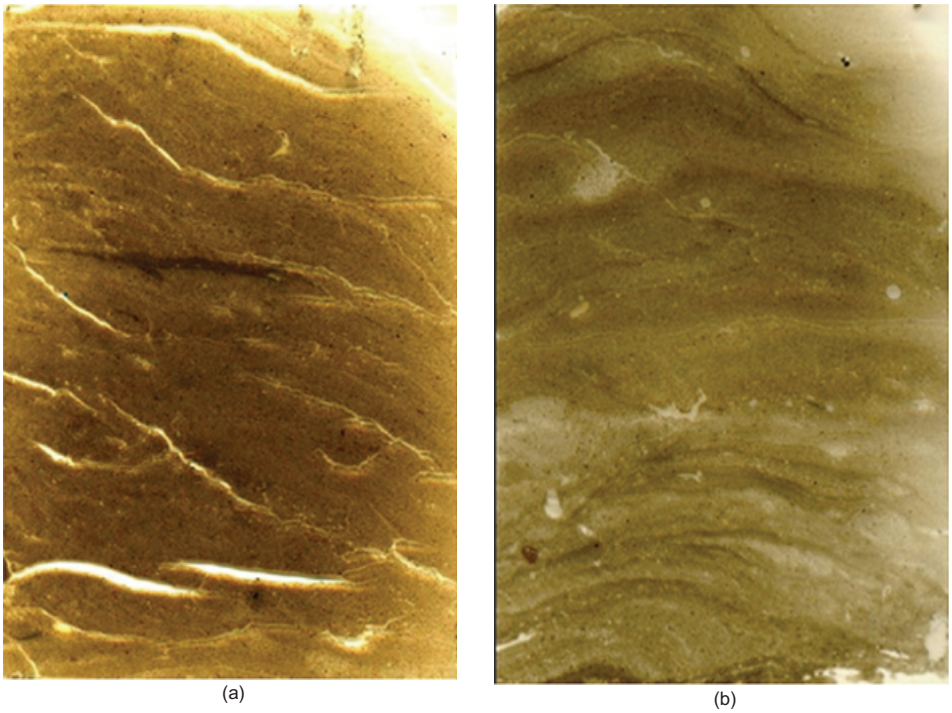

Fig. 6. Thin sections showing: (a) cracking in the LPL before treatment; (b) sealing of cracks in the LPL after precipitation applied during the winter cycle in the CCP cap

in OM and had less clay content, and thus, it did not develop desiccation cracking and a successive formation of free-flow channels that were present in the SSL and LPL. However, after the summer drought, the TSL became loose and disintegrated as individual particles. In the autumn precipitation cycle, the HC of the CCP model decreased slightly from $1{\cdot}29 \times 10^{-7}$ to $1{\cdot}16 \times 10^{-7}$ m/s due to the increased precipitation (Fig. 7). However, the NP model showed a small increase in HC due to less precipitation compared to the CCP model. This could have been due to the influence of crack formation or grass root growth with time or the combination of both. Owing to the equal amount of roots mass in both TSLs, similar patterns of HC changes were observed in both layers.

Subsoil layers. Comparison of thin sections from the NP and CCP models collected before and after the winter cycle revealed a reduction in macro-pores in the SSL due to the winter rainfall (typical mean monthly winter rainfall of 97 mm) (Figs 8(a) and 8(b)), especially in the CCP model where cracks with widths of 500–2000 μm reduced greatly after the initial wetting (Fig. 8(b)). The NP model exhibited a greater increase in HC from $2{\cdot}57 \times 10^{-10}$ m/s to $1{\cdot}96 \times 10^{-9}$ m/s than the CCP model, which was an order of magnitude higher, after the winter precipitation cycle; whereas a small increase was observed in the HC of the CCP model (from $2{\cdot}55 \times 10^{-10}$ m/s to $7{\cdot}03 \times 10^{-10}$ m/s) (Fig. 7(b)). The soil in the SSL of the CCP model could have swollen more than that in the NP model due to the relatively heavy wetting from the increased rainfall in the CCP model (Miller *et al.*, 1998). Similar changes between the total pore area and the HC were observed in the SSLs of both cap models after the winter and spring precipitation cycles.

During the spring cycle, more roots penetrated into the subsoil, which could have resulted in a greater pore area of cracks with widths 100 to >2 mm in the NP model than what was observed in the CCP model. Crack pore areas wider than 2000 μm increased by 15% and 25% in CCP and NP models, respectively. Samples collected at the end of the spring precipitation cycle showed further increase in the HCs of both cap models. However, unlike the LPLs, SSLs of both caps showed great increase in HC by an order of magnitude in this cycle. Relatively lower precipitation on both cap models during this cycle accelerated the growth of grass roots further into the SSL, as they searched for moisture, as proposed by Hauser (2008). Continuous penetration of grass roots into the SSLs aided desiccation and created free-flow channels into the SSLs, which increased HC (Miller *et al.*, 1998).

The NP model also had cracks with widths greater than 500 μm as a result of desiccation from the drought in the summer cycle. However, unlike the CCP model, cracks with widths of less than 200 μm were still present after the summer cycle. Even though the NP model experienced 80 mm of rainfall during the summer cycle, it still had an

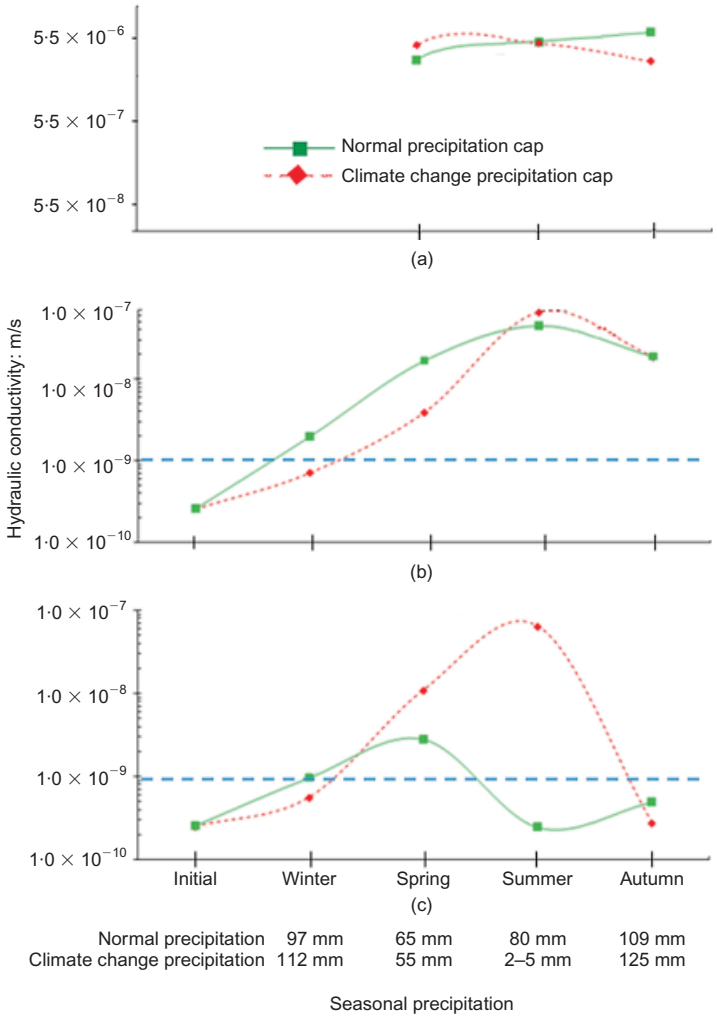

Fig. 7. Change in hydraulic conductivity in (a) topsoil, (b) subsoil and (c) low-permeability layer over the different seasons

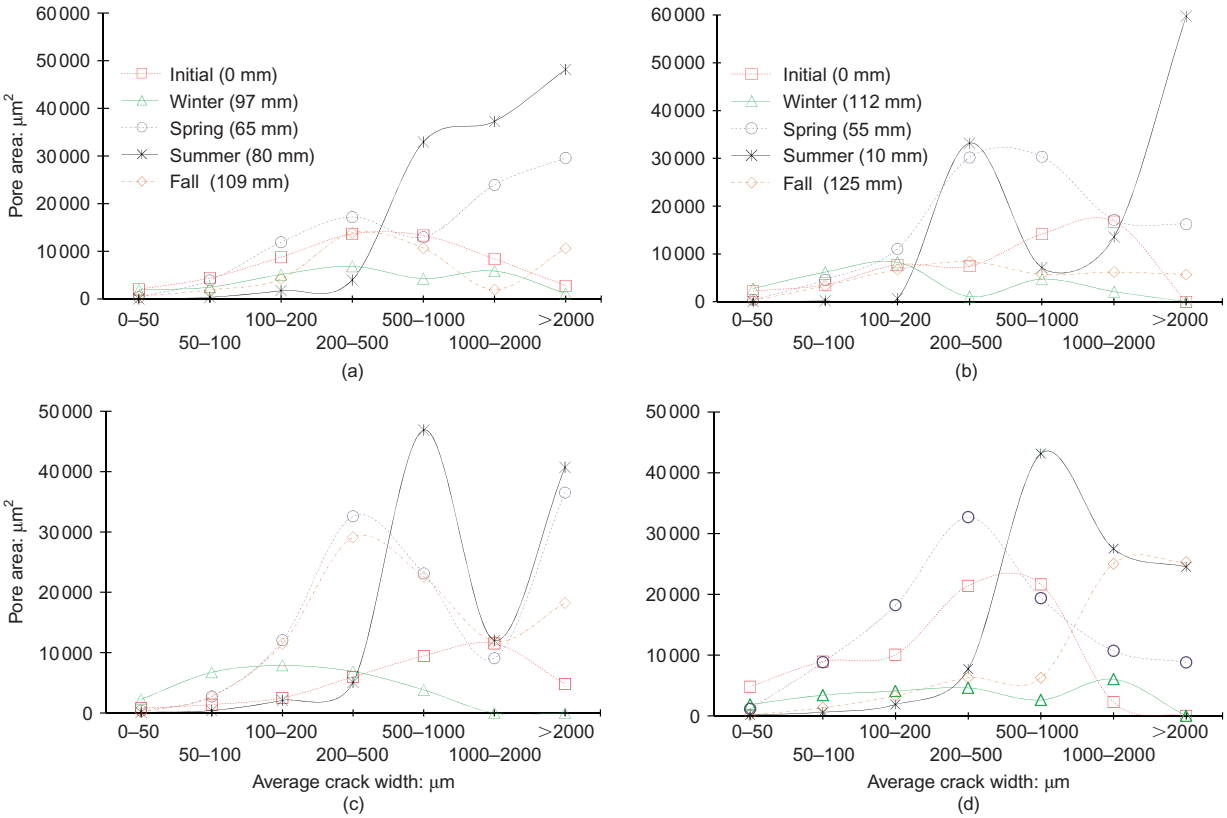

Fig. 8. Distribution of crack formation based on pore area against average crack width for: (a) NP SSL; (b) CCP SSL; (c) NP LPL; (d) CCP LPL

increase in HC from $1{\cdot}65 \times 10^{-8}$ m/s to $4{\cdot}42 \times 10^{-8}$ m/s (Fig. 7(b)). This may have resulted from continuous growth of grass roots, which eventually created water movement pathways and blocked resealing of cracks, resulting in increased HC. Total pore area in both cap models during this cycle increased (Figs 9(a) and 9(b)). In the NP model, crack pore area wider than 500 μm increased from 67% to 95%, helping to increase HC (Fig. 9(a)). After the intense summer drought experienced by the CCP model, no cracks were observed with widths less than 100 μm in the SSL. This could be because the desiccation widened the minor cracks observed in the previous cycles (Miller *et al.*, 1998), creating cracks with widths greater than 2 mm. The heavy drought experienced by the CCP model during this cycle increased the HC further by an order of magnitude from $3{\cdot}85 \times 10^{-9}$ m/s to $6{\cdot}52 \times 10^{-8}$ m/s (Fig. 7(b)) due to the formation of crack pore areas wider than 500 μm, which increased drastically from 15% to 52% (Fig. 8(b)).

Excessive precipitation in the autumn cycle, following the drought, could have caused the OM and smectite clay minerals to swell and seal cracks, reducing the amount of cracks with widths greater than 1 mm; nevertheless, cracks greater than 2 mm were still present that did not seal. Crack pore area wider than 500 μm significantly reduced in both cap models from 70% to 49% in the CCP model and 95% to 53% in the NP model (Fig. 9(a)). Consequently, HCs of the CCP and NP models decreased from $6{\cdot}52 \times 10^{-8}$ to $1{\cdot}85 \times 10^{-8}$ m/s and from $4{\cdot}42 \times 10^{-8}$ to $1{\cdot}85 \times 10^{-8}$ m/s, respectively, but stayed at two orders higher than the initial value at 10^{-10} m/s (Fig. 7(b)). The initial drying of soils creates irreversible changes in the soil fabric (Yong & Warkentin, 1975). In soils with lower clay fraction, even after heavy wetting it is almost impossible to recover the original properties. Wetting cycles could heal some minor cracks, but these remain weak zones and can be easily reopened in subsequent dry cycles (Yesiller *et al.*, 2000). Additionally, extensive root growth in the SSL, either by creating void space for water percolation or by hindering the sealing of cracks into which they have grown, could have increased the HC. Also, Ng & Zhan (2007) demonstrated that evapotranspiration of grass will produce a high soil suction deep in the soil layers, facilitating crack development and preventing the resealing of cracks.

Low permeability layer. Soon after model construction, most of the pore space in the LPL of the CCP and NP models, was in the form of fissures that were 3–2450 μm wide (typically >500 μm). Both LPLs showed similar HCs (CCP $2{\cdot}54 \times 10^{-10}$ m/s and NP $2{\cdot}58 \times 10^{-10}$ m/s), illustrating that the LPLs of both cap models were close to identical (Fig. 7(c)).

Crack classification of the LPL from both cap models shows that after the winter precipitation cycle, the majority of the pore area was occupied by pores and fissures, with widths of 500 μm or less (Figs 8(c) and 8(d). This reduction in larger cracks could have been caused by the swelling of smectite clay minerals (Miller *et al.*, 1998) or OM in the soil matrix which closed the macro-pores and kept the increase in the HC of the LPL of the CCP model, from $2{\cdot}54 \times 10^{-10}$ m/s to $5{\cdot}67 \times 10^{-10}$ m/s, lower than the HC of the NP model, which increased from $2{\cdot}58 \times 10^{-10}$ m/s to $9{\cdot}73 \times 10^{-10}$ m/s. However, in thin sections from the CCP model after the winter cycle, pore area was evenly distributed with less pore area of 5000 μm² among all the crack width classes, with fissures at a maximum of 1165 μm wide (Fig. 8(d)).

A 15% reduction in the spring rainfall in the CCP model, compared to the NP model, resulted in relatively higher

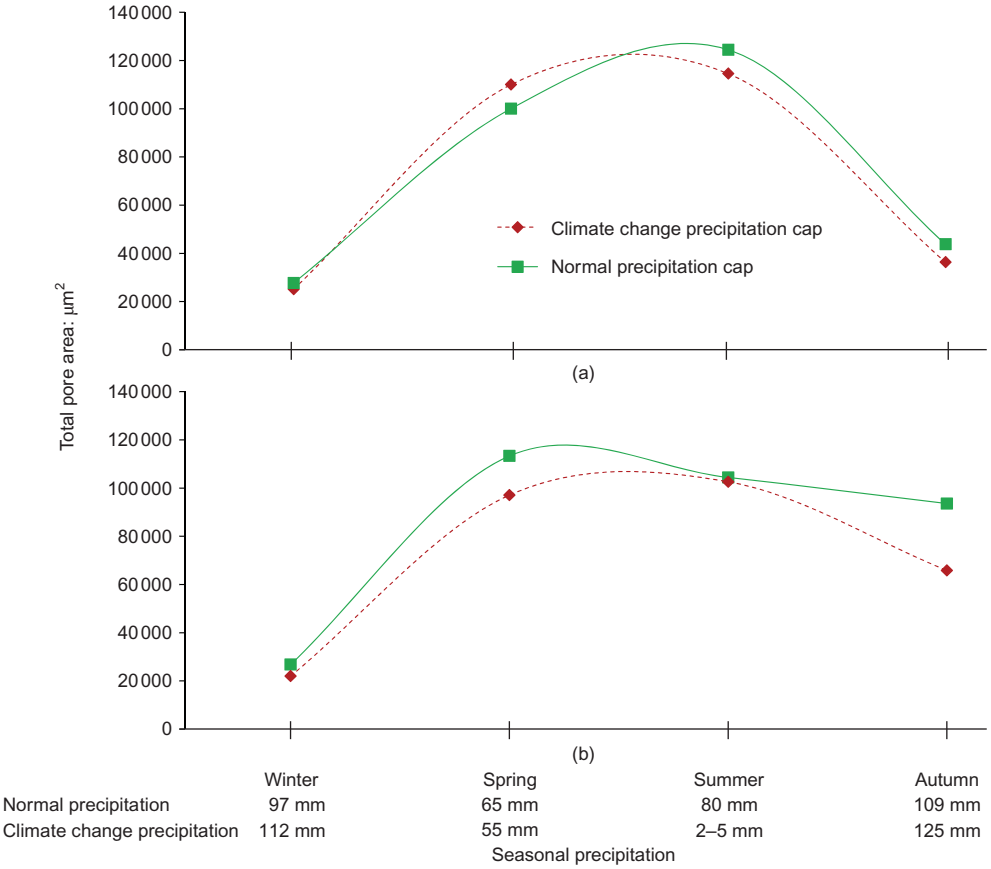

Fig. 9. Distribution of pores/cracks based on total pore area plotted against seasonal precipitation: (a) subsoil layer; (b) low-permeability layer

moisture loss from the LPL of the CCP model. The pore area increase in crack width class 100–500 μm in the LPL of the CCP model reflects the observations reported by Miller *et al.* (1998), who state that when a clay barrier layer is subjected to cyclic wetting and drying, cracks tend to appear in the area of weak planes where swelling healed the previous cracks. After spring precipitation, the crack pore area with widths of 500 μm or greater increased from 14% to 59% in the NP model. The CCP model had a pore area with widths of 2000 μm or more, which increased from 0% to 8%. In the spring precipitation event, there was a striking change in the HC of the CCP model from $5{\cdot}67 \times 10^{-10}$ m/s to $1{\cdot}09 \times 10^{-8}$ m/s, while in the NP model it was from $9{\cdot}73 \times 10^{-10}$ m/s to $2{\cdot}83 \times 10^{-9}$ m/s (Fig. 7(c)). The increment change by two orders of magnitude in the HC of the CCP model could have been caused by possible shrinkage of the smectite and OM in this cycle and an increase in desiccation cracks, as observed in the thin sections (Fig. 6(a)) (15% deficit in the mean monthly precipitation). Importantly, at the end of the winter precipitation treatment, the LPL from the CCP model failed to satisfy the guidance HC criterion of 10^{-9} m/s. However, even though the HC of the LPL from the NP model increased by an order of magnitude from 10^{-10} to 10^{-9} m/s, it satisfied the minimum HC criterion of landfill barrier layers.

As a result of 3 months' continuous summer drought, the HC of the CCP model showed a further increase from $1{\cdot}09 \times 10^{-8}$ m/s to $6{\cdot}34 \times 10^{-8}$ m/s (Fig. 7(c)). This is consistent with the total pore area change of the CCP model where the total crack pore area wider than 500 μm increased to 91% from 39% and these cracks went deeper into the soil as compared to the previous cycle. Continuous droughts could cause severe desiccation cracks, which would eventually increase the pore area of the clay barriers (Albright *et al.*, 2004). Miller *et al.* (1998) also reported that the dimension of the cracks increased in proportion to the number of wetting and drying cycles to which the clay barrier was subjected. However, crack pore area wider than 2000 μm is only 14%, which could have restricted the increase in HC over the previous cycle (end of spring cycle). The NP model which underwent typical summer precipitation (80 mm) showed a decrease from $2{\cdot}83 \times 10^{-9}$ m/s to $2{\cdot}47 \times 10^{-10}$ m/s. The applied mean monthly precipitation in the summer season on the NP model was relatively higher than the mean monthly precipitation in the spring (65 mm), which wet the LPL again and resulted in closure of small macro-cracks and decreased pore area, as seen in thin sections, which may be responsible for an HC decrease. However, crack pore area wider than 500 μm increased from 59% to 93% and cracks were deeper in the soil, which contradicts the decrease in HC. This could be due to the irreversible changes that occurred in the LPL of the NP model in the spring cycle and the continuous development of weaker planes (Yong & Warkentin, 1975). Fig. 8(d) also shows that pores created by the drought conditions in the CCP model were reduced by the successive autumn precipitation, but cracks with widths greater than 1000 μm were still present.

The autumn precipitation event provided moisture that helped to reduce the total pore areas further in both cap models; however, total pore area did not return to values similar to the winter precipitation event, as in the SSL. In the autumn precipitation cycle, the NP model was subjected to 15% less precipitation than the CCP model which increased the HC from $2{\cdot}47 \times 10^{-10}$ m/s to $4{\cdot}98 \times 10^{-10}$ m/s (Fig. 7(c)). More interestingly, the increased mean monthly precipitation in the CCP (125 mm) model decreased the HC from $6{\cdot}34 \times 10^{-8}$ m/s to $2{\cdot}80 \times 10^{-10}$ m/s, which could have resulted from the possible closure of micro- and

macro-cracks due to the swelling of smectite and OM upon wetting (Miller *et al.*, 1998; Yesiller *et al.*, 2000) as observed in thin sections. The subsequent simulated autumn precipitation event reduced the amount of cracks with widths greater than 1 mm; nevertheless, cracks greater than 2 mm were still present in the NP cap. The total pore area in the CCP model did notably reduce more than that in the NP model after the autumn precipitation. In the LPL of the CCP cap, after the simulated autumn precipitation, the majority of the pore area was in the form of cracks with a width range of 100–1000 μm, which was smaller than the width range of the cracks that occupied the majority of pore area in the previous cycle (end of summer cycle). However, as observed in the CCP model, there were cracks present with an average width of greater than 2000 μm, but they were not as prevalent, indicating a stable stage or irreversible cracking as reported by Miller *et al.* (1998). The 15% increased precipitation (125 mm) in the CCP model during the autumn cycle was unable to heal the wide-open desiccation cracks with widths greater than 1000 μm that had formed during the summer cycle. Therefore, a stable stage or irreversible cracking had developed where there was no great change in cracking. Thinner cracks created by the drought conditions were reduced by the autumn precipitation. Miller *et al.* (1998) report disappearance of cracks in a clay barrier layer (landfill cap LPL) which was subjected to cycles of wetting and drying.

After four seasonal cycles, at the end of the testing period there were no major changes observed between the original and final HCs of the LPLs for both cap models. The LPL of the NP model showed small changes where the HC fluctuated by an order of a magnitude after four seasonal precipitation cycles. Even though the CCP model experienced great fluctuations over time (maximum of two orders of magnitude), it returned to the original value of 10^{-10} m/s. This recovery could be due to gypsum infilling and clogging smaller cracks in the LPL of both cap models after the autumn cycle. The difference in the total pore area and HC values at the end of the study may also be related to gypsum infilling in smaller cracks and pores (Fig. 10(a)), although these crystals were observed creating small cracks in the matrix as they formed (Fig. 10(b)). Sulfate-rich water produced from the oxidation of pyrite (Fig. 10(c)) was neutralised by calcium carbonate shell material (Fig. 10(d)) which resulted in the formation of these gypsum crystals (selenite) in the SSL and LPL in this study. Pyrite and shell material

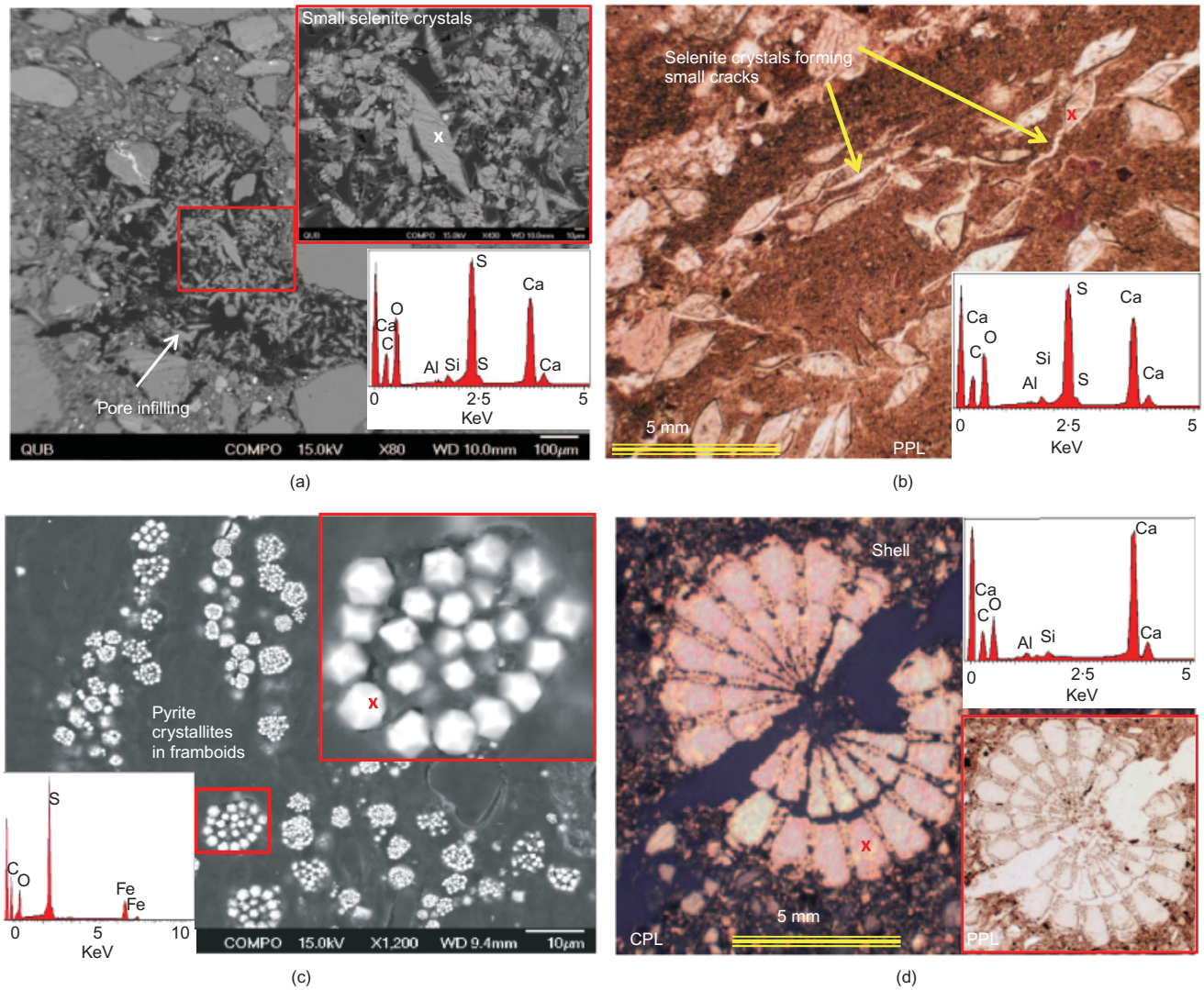

Fig. 10. (a) SEM micrograph showing a pore in which small selenite crystals have formed and SEM-EDS spectrum of the elemental composition of a crystal; (b) single selenite crystals forming small cracks in the LPL of the NP cap after the spring precipitation cycle and SEM-EDS spectrum of the elemental composition of a crystal. (c) SEM micrograph of small pyrite crystallites within framboids with SEM-EDS spectrum showing elemental composition of a framboid; (d) micrograph of a small shell in PPL and CPL with SEM-EDS spectrum showing elemental composition of the shell (PPL, plane polarised light; CPL, cross polarised light)

are plentiful in Belfast Sleech. Additionally, this study shows that image analysis of desiccation cracks in thin sections is very useful in studying the behaviour of smaller cracks (i.e. < 2 mm), but it may not be completely representative of crack formation and behaviour in a landfill cap. Therefore, in order to examine the development of larger cracks and their effect on HC, a broader based study is needed which incorporates visual observations along with other field and laboratory analysis.

CONCLUSIONS

In this study, a fine-textured Belfast Sleech was used as capping material because it is easily compactable below the permeability limit for landfill caps, fairly uniform in composition, contains smectite clays which can aid in resealing desiccation cracks, and meets the guidelines for capping material. However, the formation of desiccation cracks from extreme simulated drought and rainfall events, based on future climate change scenarios for southwest England, destroyed the overall integrity of landfill capping layers in a large-scale physical model, whereas a landfill model that received normal climate precipitation retained its integrity over the 1-year testing period. Also, grass root growth into desiccation cracks hindered resealing, especially in the climate change model. The Belfast Sleech in the LPL has a high (~6%) OM content and if cracks form that do not reseal, the OM can oxidise away over time, which will further enlarge the cracks and prevent resealing. Interestingly, gypsum formation in the SSL and LPL of both models appeared to be brought on by precipitation events. Along with swelling of clays and OM in the LPL, it is hypothesised that gypsum crystallisation in pores and cracks in the LPL could have aided in the lowering of the HCs in both caps to near the original values, below the permeability limits for landfill caps, thereby exhibiting resealing capabilities for small cracks. Other processes not investigated here may also be involved. It is worth mentioning that these findings are specific to the soil type used. Caps using other soil types may behave differently.

Although this research was conducted under typical and projected climate change precipitation events for north-west England, the findings are applicable to the impacts of climate change precipitation on landfill caps globally. The study shows that dry periods in a possible future climate could lead to significant deterioration of cap performance. It has also provided insight into some of the mineralogical processes that may be driving such changes in performance (e.g. swelling of smectite and formation of gypsum crystals) and the interplay with root growth. Selection of landfill capping material should be carefully considered beyond just meeting permeability requirements at the time of placement. Additionally, it is advisable to carry out preliminary mineralogical tests and to select cover vegetation that does not have aggressive root development, which would hinder resealing of desiccation cracks. This information needs to be taken into consideration in landfill cap material selection and design stages, especially for landfill caps that will be used to cover hazardous waste disposal sites over lengthy periods, which may be subject to predicted climate change scenarios. Longer-term studies are needed to give clearer insights into the desiccation cracking and resealing abilities of different materials that could be used as clay barriers in subsequent wetting cycles and associated HC changes.

ACKNOWLEDGEMENTS

This project was funded by a Nuclear Decommissioning Authority PhD bursary and thin sectioning equipment was funded by an Engineering and Physical Science Council equipment grant. The authors thank Agri-Food and Bioscience Insitute Northern Ireland for allowing the experiment to be carried out in their greenhouse and for their continued support for the duration of the project.

REFERENCES

Albright, W., Benson, C. H., Gee, G. W., Roesler, A., Abichou, T., Preecha, A., Bradley, F. & Rock, S. A. (2004). Field water balance of landfill final covers. *J. Environ. Qual*. **33**, No. 6, 2317–2332.

Albright, W. H., Benson, C. H., Gee, G. W., Abichou, T., McDonald, E. V., Tyler, S. W. & Rock, S. A. (2006). Field performance of a compacted clay landfill final cover at a humid site. *J. Geotech. Geoenviron. Engng* **132**, No. 11, 1393–1403.

Anderson, C. (2011). *The permeability of fine grained soils: An investigation into unconventional methods of measurement in the laboratory.* PhD thesis, Queen's University, Belfast, UK.

Basnett, C. & Bruner, R.. (1993). Clay desiccation of a single composite liner system. *Proceedings of geosynthetics '93, Industrial Fabrics Association, St Paul, Minnesota*, pp. 1329–1340.

Basnett, C. & Brungard, M. (1992). The clay desiccation of a landfill composite lining system. *Geotech. Fabrics Rep. IFAI* **10**, No. 1, 38–41.

Bending, N. A. D. & Moffat, A. J. (1997). *Tree establishment on landfill sites. Research and updated guidance*. Edinburgh, UK: DETR, Forestry Commission.

Boivin, P., Garnier, P. & Tessier, D. (2004). Relationship between clay content, clay type, and shrinkage properties of soil samples. *Soil Sci. Soc. Am. J.* **68**, No. 4, 1145–1153.

Bowders, J. J., Daniel, D. E., Wellington, J. & Houssidas, V. (1997). Managing desiccation cracking in compacted clay liners beneath geomembranes. *Proceedings of geosynthetics '97, NAGS, Long Beach*, pp. 527–540.

Boynton, S. S. & Daniel, D. E. (1985). Hydraulic conductivity tests on compacted clay. *J. Geotech. Geoenviron. Engng* **111**, No. 4, 465–478.

BSI (1990a). BS 1377-2: Methods of test for soils for civil engineering purposes. Determination of particle size. Method 9.2. London, UK: BSI.

BSI (1990b). BS 1377-6: Methods of test for soils for civil engineering purposes. Consolidation and permeability tests in hydraulic cells and with pore pressure measurement, p. 74. London, UK: BSI.

Corser, P. & Cranston, M. (1991). Observations on long-term performance of composite clay liners and covers. In *Proceedings of geosynthetics design and performance conference, Vancover, Canada*. Vancouver, Canada: British Columbia Geotechnical Society.

Costa, S., Kodikara, J. & Shannon, B. (2013). Salient factors controlling desiccation cracking of clay in laboratory experiments. *Géotechnique* **63**, No. 1, 18–29, http://dx.doi.org/10.1680/geot.9.P.105.

Crooks, J. H. A. & Graham, J. (1976). Geotechnical properties of the Belfast estuarine deposits. *Géotechnique* **26**, No. 2, 293–315, http://dx.doi.org/10.1680/geot.1976.26.2.293.

Defra (Department of the Environment, Food and Rural Affairs) (2009). *UKCP 09 climate projection model*. London, UK: Defra. See http://ukcp09.defra.gov.uk (accessed 08/12/2013).

Driscoll, R. (1983). The influence of vegetation on the swelling and shrinking of clay soils in the Britain. *Géotechnique* **33**, No. 2, 93–105, http://dx.doi.org/10.1680/geot.1983.33.2.93.

Fitzpatrick, E. A. (1993). *Soil microscopy and micromorphology.* New York, NY, USA: Wiley.

Glossop, N. H. & Farmer, I. W. (1979). Sediment associated with removal of compressed air pressure during tunnelling in alluvial clay. *Géotechnique* **29**, No. 1, 67–72, http://dx.doi.org/10.1680/geot.1979.29.1.67.

Greenway, D. R. (1987). Vegetation and slope stability. In *Slope stability* (eds M. F. Anderson and K. S. Richards). New York, NY, USA: Wiley.

Hauser, V. L. (2008). *Evapotranspiration covers for landfills and waste sites*. Boca Raton, FL, USA: CRC Press.

Holtz, W. G. (1983). The influence of vegetation on the swelling and shrinking of clays in the United States of America.

Géotechnique **33**, No. 2, 159–163, http://dx.doi.org/10.1680/geot.1983.33.2.159.

Hutchings, T. R., Moffat, A. J. & Kemp, R. A. (2001). Effects of rooting and tree growth of selected woodland species on cap integrity in a clay capped landfill site. *Waste Manage. Res.* **19**, No. 3, 193–200.

Jones, R. M., Murray, E. J., Rix, D. W. & Humphrey, R. D. (1993). Selection of clays for use as landfill liners. In *Proceedings of GREEN '93 – An international symposium on geotechnics related to the environment, Bolton*. Rotterdam, the Netherlands: Balkema.

Lim, T. T., Rahardjo, H., Chang, M. F. & Fredlund, D. G. (1996). Effect of rainfall on matric suctions in a residual soil slope. *Can. Geotech. J.* **33**, No. 4, 618–628.

MacLeod, G. (2008). *Soil thin sections and preparation*. Scotland, UK: University of Stirling. See http://www.thin.stir.ac.uk (accessed 18/12/2013).

Melchior, S. (1997). In-situ studies of the performance of landfill caps (compacted soil liners, geomembranes, geosynthetic clay liners and capillary barriers). *Land Contamin. Remediation* **5**, No. 3, 209–216.

Melchior, S., Berger, K., Vielhaber, B. & Miehlich, G. (1994). Multilayer landfill covers: Field data on the water balance and liner performance. In *In-situ remediation: scientific basis for current and future technologies* (eds G. W. Gee and N. R. Wing), pp. 411–425. Columbus, OH, USA: Battelle Press.

Melchior, S., Sokollek, V., Berger, K., Vielhaber, B. & Steinert, B. (2010). Results from 18 years of in situ performance testing of landfill cover systems in Germany. *J. Environ. Engng* **136**, No. 8, 815–823.

Miller, C. J. & Mishra, M. (1989). Modeling of leakage through cracked clay liners – I: state of the art. *Wat. Resour. Bull*. **25**, No. 3, 551–555.

Miller, C. J., Mi, H. & Yesiller, N. (1998). Experimental analysis of desiccation crack propagation in clay liners. *J. Am. Wat. Resour. Assoc*. **34**, No. 3, 677–686.

Montgomery, R. & Parsons, L. (1989). The Omega Hills final cover test plot study: Three year data summary. *Proceedings of the 1989 annual meeting of the National Solid Waste Management Association, Washington D.C*., pp. 1–14.

Ng, C. W. W. & Zhan, L. T. (2007). Comparative study of rainfall infiltration into a bare and a grassed unsaturated expansive soil slope. *Soils Found*. **47**, No. 2, 207–217.

NRA (National Rivers Authority) (1992). *Policy and practice in the protection of groundwater*. Bristol, UK: NRA.

Phillips, D. H. & FitzPatrick, E. A. (1999). Biological influences on the morphology and micromorphology of selected Podzols (Spodosols) and Cambisols (Inceptisols) from the Eastern United States and Northeast Scotland. *Geoderma* **90**, No. 3–4, 327–364.

Phillips, D. H. G., Sinnathamby Russell, M. I., Anderson, C. & Pasky, A. (2011). Mineralogy of selected geological deposits from the Republic of Ireland and the United Kingdom for possible use as landfill capping materials for low-level radioactive waste facilities. *Appl. Clay Sci*. **53**, No. 3, 395–401.

Rayhani, M. H. T., Yanful, E. K. & Fakher, A. (2008). Physical modeling of desiccation cracking in plastic soils. *Engng Geol*. **97**, No. 1, 25–31.

SEPA (Scottish Environment Protection Agency) (2002). *Framework for risk assessment for landfill sites: The geological barrier, mineral layer and the leachate sealing and drainage system. Version 10*. Stirling, Scotland, UK: SEPA.

Sinnathamby, G. (2011) *Hydraulic conductivity and porosity changes in landfill cap models in response to climate change*. PhD thesis, Queen's University Belfast, UK.

Tang, C., Shi, B., Liu, C., Zhao, L. & Wang, B. (2008). Influencing factors of geometrical structure of surface shrinkage cracks in clayey soils. *Engng Geol*. **101**, No. 3–4, 204–217.

Tay, Y. Y., Stewart, D. I. & Cousens, T. W. (2001). Shrinkage and desiccation cracking in bentonite-sand landfill liners. *Engng Geol*. **60**, No. 1–4, 263–274.

Vallejo, L. E. (2009). Fractal analysis of temperature-induced cracking in clays and rocks. *Géotechnique* **59**, No. 3, 283–286, http://dx.doi.org/10.1680/geot.2009.59.3.283.

Yesiller, N., Miller, C. J., Inci, G. & Yaldo, K. (2000). Desiccation and cracking behavior of three compacted landfill liner soils. *Engng Geol*. **57**, No. 1–2, 105–121.

Yong, R. W. & Warkentin, B. P. (1975). *Soil properties and behaviour*. New York, NY, USA: Elsevier.